PERGAMON

Deep-Sea Research I 48 (2001) 1793–1819

DEEP-SEA RESEARCH
PART I

www.elsevier.com/locate/dsr

Transport of newly ventilated deep water from the Iceland Basin to the Westeuropean Basin

Uli Fleischmann[a,*], Hauke Hildebrandt[b], Alfred Putzka[a], Reinhold Bayer[b]

[a]*Institut für Umweltphysik, Universität Bremen, Postfach 330440, D-28334 Bremen, Germany*
[b]*Institut für Umweltphysik, Universität Heidelberg, Im Neuenheimer Feld 229, D-69120 Heidelberg, Germany*

Received 26 June 2000; received in revised form 29 November 2000; accepted 5 December 2000

Abstract

Increased values of trichlorofluoromethane (CFC-11), tritium and stable tritium in the depth range from 2500 to 3500 m at the eastern flank of the Mid-Atlantic Ridge at 48°N (WHP section A2) indicate an influence of newly ventilated water. Water with similar Θ, S and tracer properties is found on the WHP section A1 (55°N) situated north of the Gibbs Fracture Zone in the Iceland Basin. The high tracer concentrations are due to the influence of Iceland Scotland Overflow Water (ISOW). The ISOW-influenced water found in the Iceland Basin partially passes by the Gibbs Fracture Zone (52°N) and flows southward along the topography of the Mid-Atlantic Ridge. A quantitative analysis of the transport from the Iceland Basin to the Westeuropean Basin is carried out based on the assumption that the water with enhanced tracer values is a two-component mixture of recirculating North East Atlantic Deep Water from the eastern part of the Westeuropean Basin and ISOW-influenced water as found on A1 in the Iceland Basin ($NEADW_{IB}$). The composition of the mixture and the transport time for the $NEADW_{IB}$ are deduced from the temporal evolution of the tracer values. From the distance between the two sections and the area with enhanced tracer values, a transport of $NEADW_{IB}$ from the Iceland Basin to the Westeuropean Basin of 1.63 ± 0.32 Sv[1] is calculated for the density range $41.37 < \sigma_3 < 41.475$. Transports between 2.4 and 3.5 Sv result if the transport in the former density range is extrapolated to $41.35 < \sigma_3 < 41.52$ (corresponding to $\sigma_\Theta > 27.8$) in different ways.

Keywords: Tracers; Transport; Freons; Tritium; ISOW; NADW; 45–60°N; 10–30°W; North Atlantic; Westeuropean Basin

* Corresponding author. Fax: +49-(0)421-218-7018.
E-mail address: ufleisch@physik.uni-bremen.de (U. Fleischmann).

[1] $1\,\text{Sv} = 10^6\,\text{m}^3/\text{s}$.

0967-0637/01/$ - see front matter
PII: S0967-0637(00)00107-2

1. Introduction

The formation of Iceland Scotland Overflow Water (ISOW) is initiated by approximately 2 Sv of cold and dense water leaving the Norwegian Sea through the Faroe Bank Channel (Borenäs and Lundberg, 1988; Swift, 1984; Fig. 1). Surrounding warmer water is entrained on its way through the channel and as it descends from the sill depth to the level of its appropriate density. The cold and warm components mix as the water is transported through the Iceland Basin, where it follows the topography at first to the west and then southwest along the Reykjanes Ridge. By the time the water mass arrives south of Iceland, the mixture is fairly homogenous (van Aken and de Boer, 1995). This mixture is called ISOW and is characterised by high salinities. It is found mainly at depths between 1000 and 2000 m on the Icelandic Slope (63°N, 17°W; van Aken and de Boer, 1995), where it has increased its flow to 3.2 Sv (Saunders, 1995). The core lowers to 2000–3500 m at the Reykjanes Ridge (58°N, 30°W, WHP A1 section). It becomes part of the Deep Northern Boundary Current (DNBC), which is initiated by Eastern Basin Bottom Water (EBBW) (McCartney, 1992), a diluted form of Antarctic Bottom Water. The latter enters the eastern North Atlantic through the Vema Fracture Zone (11°N) and propagates north (McCartney et al., 1991) while mixing with overlying water to form the EBBW. This forms a northward flowing eastern boundary current in the eastern Basin north of the Madeira Abyssal Plain. In the Westeuropean Basin (WEB) it mixes further with recirculating Northeast Atlantic Deep Water (NEADW). Approximately 3 Sv EBBW and NEADW are reported to turn west at the northern margin of the Westeuropean Basin initiating the DNBC (Schmitz and McCartney, 1993).

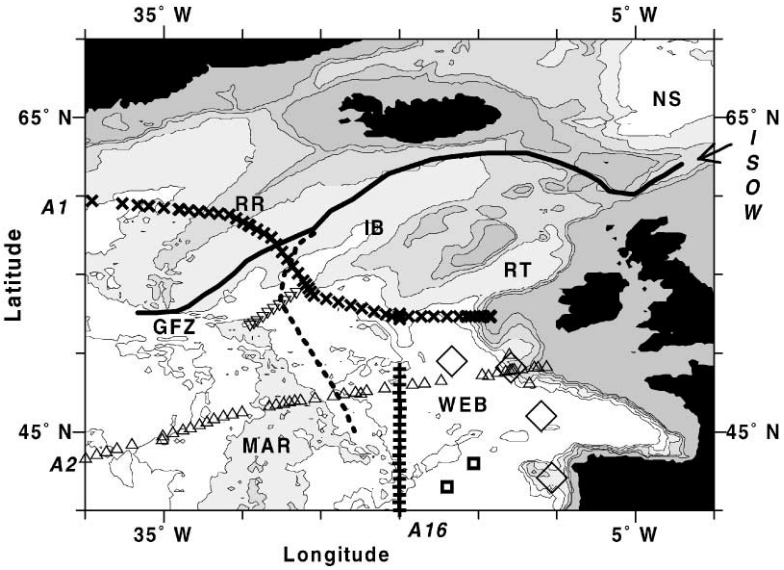

Fig. 1. Topography of the study area with cruise tracks: A1 (*Meteor* 18, 1991 and 30/3, 1994) is marked by (×), A2 (*Meteor* 30/2, 1994) by (△), A16N (*Oceanus* 202, 1988) by (+), TTO (1981) by (◇), *Meteor* 56 (1981) by (□) and *Meteor* 39/5 by (▽). The solid line indicates the traditionally believed pathway of ISOW, the dashed an additional one proved here. Isopleths are shown for 500, 1000, 2000, 3000 and 4000 m. Areas with less than 3000 m are shaded. NS = Norwegian Sea, RR = Reykjanes Ridge, IB = Iceland Basin, RT = Rockall Trough, GFZ = Gibbs Fracture Zone, MAR = Mid-Atlantic Ridge, WEB = Westeuropean Basin.

The separation of the deep eastern and deep western North Atlantic by the Reykjanes Ridge and the Mid-Atlantic Ridge is interrupted in the southwestern Iceland Basin by the Gibbs Fracture Zone (GFZ), where sill depths of more than 3500 m are found. The ISOW, as part of the DNBC, is no longer forced by the topography to flow south but can turn west into the western part of the North Atlantic. Its arrival in the western North Atlantic is frequently reported from measurements in the Irminger Basin (e.g. Dickson, 1994) where it is sometimes called Gibbs Fracture Zone Water. In studies on the circulation of the northern North Atlantic (NA) this pathway is usually reported as the only one for ISOW (e.g. McCartney, 1992; Schmitz and McCartney, 1993). But Lee and Ellet (1965) concluded from salinity anomalies that the eastern NA also receives ISOW. Smethie et al. (2000) identified ISOW in the eastern NA from high CFC-11 at a density of $\sigma_2 > 37.08$, exceeding that of the water flowing through the GFZ. They concluded that a part of the ISOW has to stay in the eastern basin. Current meters moored in the GFZ yielded a westward transport of 2.4 Sv (Saunders, 1994), which is not large enough to account for the whole DNBC transport of approximately 7 Sv. The 7 Sv results from the initial 3 Sv EBBW and NEADW transport and approximately 4 Sv ISOW and entrainment (see above).

This study is based on measurements of the transient tracers CFC-11, tritium and ^{3}He. Transient tracers are substances with a time-dependent input into the ocean. CFC-11 and tritium have a time-dependent input to the ocean primarily because their man-made production rates have changed over time (industrial production of chlorofluorocarbons (CFCs), release of bomb tritium). This makes them very suitable for the investigation of time-dependent processes. They are used, for example, to study the ventilation of the global gyre systems (e.g. Jenkins, 1988), for investigations of the thermohaline circulation (e.g. Roether et al., 1994) or to determine the spreading velocity and formation rates of water masses (e.g. Sy et al., 1997; Rhein et al., 2001).

Tracer data from the northeastern North Atlantic show clear evidence that water which is influenced by newly ventilated ISOW reaches the Westeuropean Basin. These data are used to estimate the transport of deep water from the Iceland Basin to the Westeuropean Basin.

2. Data and methods

2.1. Transient tracers and dating methods

The predominant input of the tracers used in this study takes place at the surface, from where they are transported into the ocean interior. Of the three tracers used, only CFC-11 is a stable tracer: i.e. CFC-11 concentrations are changed only by mixing with water of different CFC-11 concentrations. Tritium values change due to mixing and additionally because tritium decays radioactively to tritiugenic ^{3}He.

For trace gases such as CFCs, the concentration in surface waters is often assumed to be in equilibrium with the atmosphere. Under this assumption the surface concentrations can be calculated from the known or modelled atmospheric values (Walker et al., 2000) and the solubilities of the trace gases in seawater (Warner and Weiss, 1985).

Tritium cannot be treated in this way because it enters the water as part of water molecules. The surface water tritium concentrations have therefore been reconstructed from measurements and models by Dreisigacker and Roether (1978) and Doney and Jenkins (1988) for the time till 1981.

The surface water concentrations from 1981 to 1994 have been estimated by fitting an exponential function to surface measurements in 1988, 1991 and 1994 which fits smoothly to the function given in Doney and Jenkins (1988). In order to be able to use tritium as a conservative tracer its radioactive decay has to be considered. This is done by correcting all values for their decay to a common date (1991 in this study). The conservative quantity derived is named tritium91, with the associated unit TU91 (Doney and Jenkins, 1994).

Tritiugenic ^{3}He is the decay product of tritium. The concentration of tritiugenic ^{3}He is zero in the surface layer, because ^{3}He equilibrates with the atmosphere. ^{3}He accumulates as a water parcel moves away from the surface into the interior, where the ^{3}He from the tritium decay can no longer escape to the atmosphere. But tritium decay is not the only source for oceanic ^{3}He. The predominant source is the atmosphere, and there is additionally a terrigenic component. The tritiugenic part is separated from these two as described in Section 2.2. The concentrations of tritiugenic ^{3}He are given in TU as well. In this case 1 TU of tritiugenic ^{3}He is the amount of ^{3}He that emerges from the decay of 1 TU of tritium. The sum of tritium and tritiugenic ^{3}He is a stable tracer which is named stable tritium (Jenkins, 1998). It is the third tracer used in the mixing analysis carried out in this study.

Transient tracers are used to determine the age of water (Doney et al., 1997), which is the time since leaving the surface. This can also be thought of as the time when the final resetting of the tracer properties of the water takes place. The most simple way to estimate an age from a measured tracer value is the calculation of a concentration age. In this case it is assumed that the water from which the sample was drawn has travelled from the surface to the place of sampling without mixing with other water. The year of formation can then directly be read from the surface water history (Fig. 2).

In general, however, it is unrealistic to assume that no mixing occurs after water leaves the surface. Where a surface water mass with a tracer signature mixes with tracer-free water, the ratio of two tracers can be used in the same way as concentration dating uses the concentrations, because ratios remain unaltered when tracer-free water is admixed. Ratio dating determines the age (t) and the fraction of the young, tracer-carrying component (x_Y) from the measured concentrations of two tracers (CFC-11$_{meas}$ and tritium91$_{meas}$ in the following example). Mathematically ratio dating can be expressed by the following equations:

$$\begin{aligned} \text{CFC-11}_{meas} &= x_Y \cdot \text{CFC-11}(t), \\ \text{tritium91}_{meas} &= x_Y \cdot \text{tritium91}(t). \end{aligned} \tag{1}$$

Dividing the first equation by the second eliminates the fraction (x_Y) of the tracer-carrying young water, and the value of the ratio can be compared with the history of the ratio for the surface water (Fig. 2) to determine the year of formation (t). In addition, the fraction of young (and old) water in the mixture can be calculated from the absolute values of the tracers and the known values in the year of formation. Effects of undersaturation and mixing of different tracer-carrying waters are not considered in this dating approach nor is mixing of water from different vintages.

2.2. Data used in this study

The data used for this study are tritium, ^{3}He and CFC-11 data from the WHP sections A1, A2 and A16N. WHP A1 was occupied twice (*Meteor* cruise M 18 in 1991 and M 30/3 in 1994), the

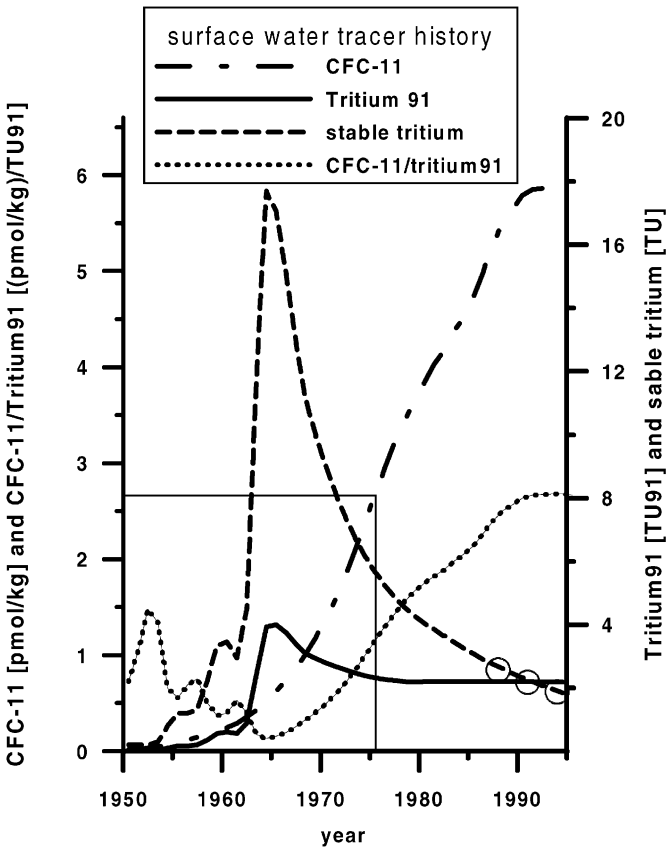

Fig. 2. Time dependency of concentrations of CFC-11 (dashed–dotted), tritium91 (solid) and stable tritium (dashed) in surface water. The CFC-11 concentrations are given for water with $\Theta = 2.95^{\circ}$C and $S = 34.93$. The tritium91 values are derived from the reconstructed surface water history for stable tritium (dashed) given in Doney and Jenkins (1988). The latter has been extrapolated for the period 1981–1994 with an exponential fit to surface measurements in 1988, 1991 and 1994 (○, the size of the circle corresponds to 4σ). The ratio of CFC-11 and tritium91 is shown as a dotted line. The determination of the concentration age for a sample measured in 1991 ($\Theta = 2.95$, $S = 34.93$) with a CFC-11 concentration of 2.6 pmol/kg is shown. This concentration of CFC-11 was reached in 1975 and thus a concentration age of 16 yr results.

WHP A2 section only in 1994 (*Meteor* 30/2). A16N was realised in 1988 (*Oceanus* cruise 202; Tsuchiya et al., 1992). The tritium and ^{3}He data have been supplemented with data from the TTO programme (Transient Tracers in the Ocean, 1981 St. nos. 114–117, ◇ in Fig. 1). Some CFC-11 measurements from an early *Meteor* cruise (M 56 in 1981, □ in Fig. 1) are added to complete the data set.

CFC-11 was measured onboard, except for M 56 (1981), where water samples were filled into evacuated fine steel containers and measured in the home laboratory. On the other cruises approximately 100 ml of water was sampled into an ampoule or a syringe. CFC-11 was extracted from the water and measured with an EC-GC system (similar to the one) described by Bullister and Weiss (1988). The system used on WHP A2 (1994) was a modified version described in Bulsiewicz

Table 1
Measurement precision for CFC-11, tritium, ^{3}He and stable tritium

CFC 11	Tritium	^{3}He	Stable tritium
0.01 pmol/kg or 1% whichever is greater	0.01 TU or 4% whichever is greater	0.5%	0.1 TU

et al. (1995). The CFC-11 values are all reported on the SIO93 scale (Cunnold et al., 1994). The measurement precision is given in Table 1.

Water samples for tritium and helium measurements were taken onboard and stored for subsequent analysis, mostly at the Institut für Umweltphysik, Heidelberg (M 18, M 30/2 and M 30/3). Water was sampled into 1 l glass bottles for tritium measurements. In the laboratory all gas was extracted from half a litre of water. The gas-free water was then stored for an appropriate length of time in order to let the tritium decay product ^{3}He grow. This was measured by mass spectrometry. For measurement precision see Table 1.

Helium samples were drawn into 40 ml copper tubing, which was clamped off and the sample stored until it was analysed. Analysis of the helium isotopes ^{3}He and ^{4}He involved extraction of the gas from the water samples and subsequent analysis using a specially designed mass spectrometer. For measurement precision see Table 1. A more detailed description of the system used for the tritium and helium measurements is given in Bayer et al. (1989).

The contributions of atmospheric and terrigenic ^{3}He have to be subtracted from the measured ^{3}He to obtain the tritiugenic ^{3}He. The atmospheric component is estimated from the measured ^{4}He (Jenkins and Clarke, 1976, p. 490) using the atmospheric mixing ratio considering the helium isotope effect in solution (Benson and Krause, 1980). Excess ^{3}He results from the subtraction of this atmospheric ^{3}He from the measured ^{3}He. Non-atmospheric parts in the ^{4}He concentration are neglected and the excess ^{3}He is therefore only approximately the sum of the terrigenic and tritiugenic components. The terrigenic contribution is mainly imported by Antarctic Bottom Water, which has high silica concentrations as well. The terrigenic component can therefore be estimated in the deep North Atlantic from its correlation with silica as shown by Doney and Jenkins (1994).

Vertical sections of CFC-11 in the deep eastern basin on A1 (1991) and A2 (1994) are presented as examples for tracer distributions in the deep northeastern North Atlantic (Fig. 3). The overall structure is dominated by the contrast between the high CFC levels in the Labrador Sea Water at depths of 1000–1500 m and the low CFC levels of the Eastern Basin Bottom Water at the bottom of the easternmost parts of the sections. For the A1 section, the influence of ISOW is clearly visible as a CFC maximum at the bottom of the water column above the eastern flank of the Reykjanes Ridge (Fig. 3a). On the A2 section, the ISOW influence is no longer strong enough to develop a bottom maximum but it causes an inclination of the isolines in the deep water, rising from west to east (Fig. 3b).

Θ-S diagrams and Θ-tracer plots are shown in Fig. 4 for the section A2 and in Fig. 5 for the section A1. The salinities are reported according to the practical salinity scale. The tracer values of the WHP A2 section in 1994 at the stations close to the eastern flank of the Mid-Atlantic Ridge (MAR) (Fig. 4, +) are higher for $2.4^\circ C < \Theta < 3.2^\circ C$ compared to values at stations further east

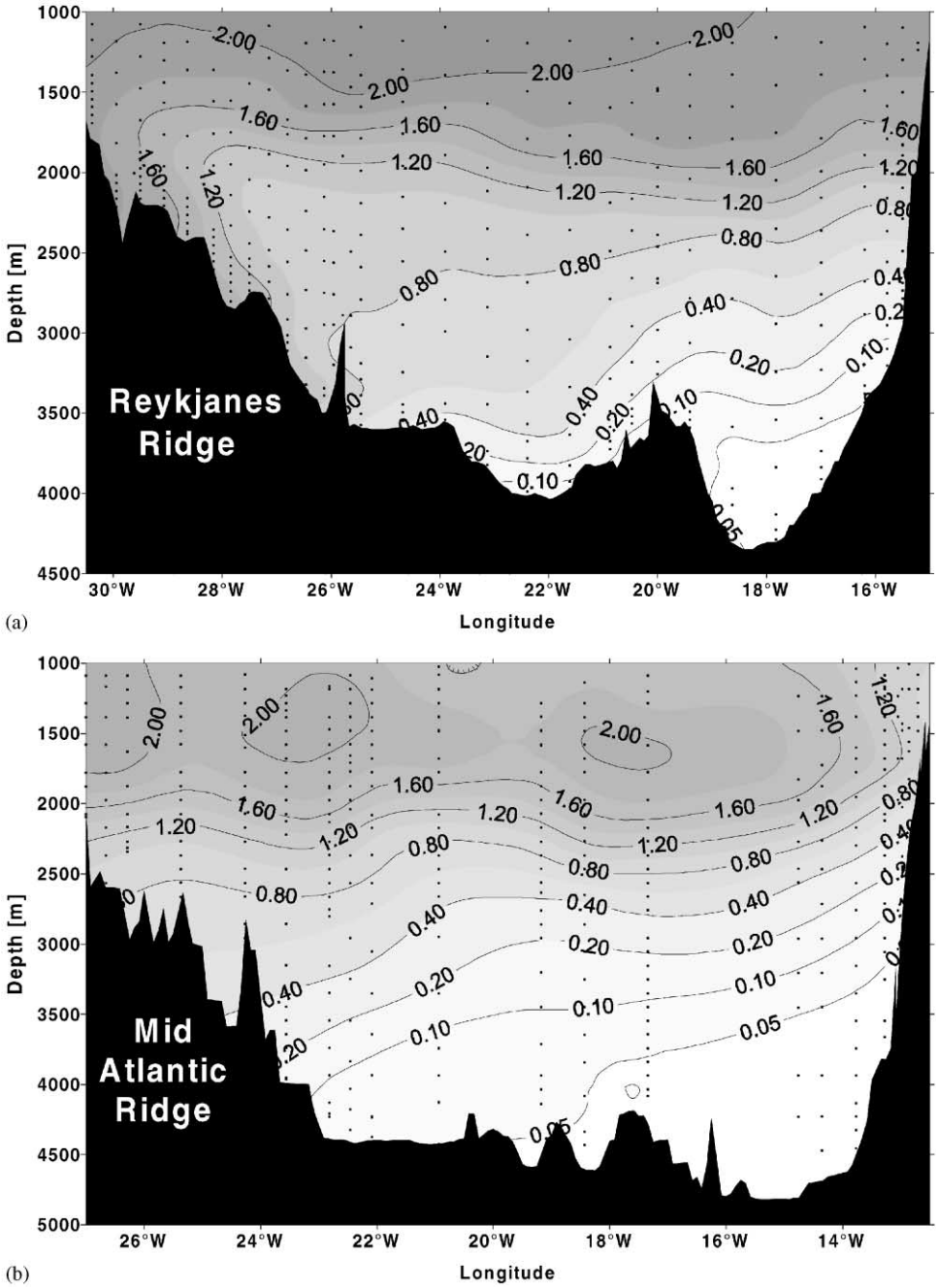

Fig. 3. Vertical sections of CFC-11 [pmol/kg] for the deep eastern part of WHP A1 in 1991 (a) and for the deep eastern part of WHP A2 in 1994 (b). The presence of ISOW is responsible for the bottom maximum at the Reykjanes Ridge on A1 and inclined isolines on A2.

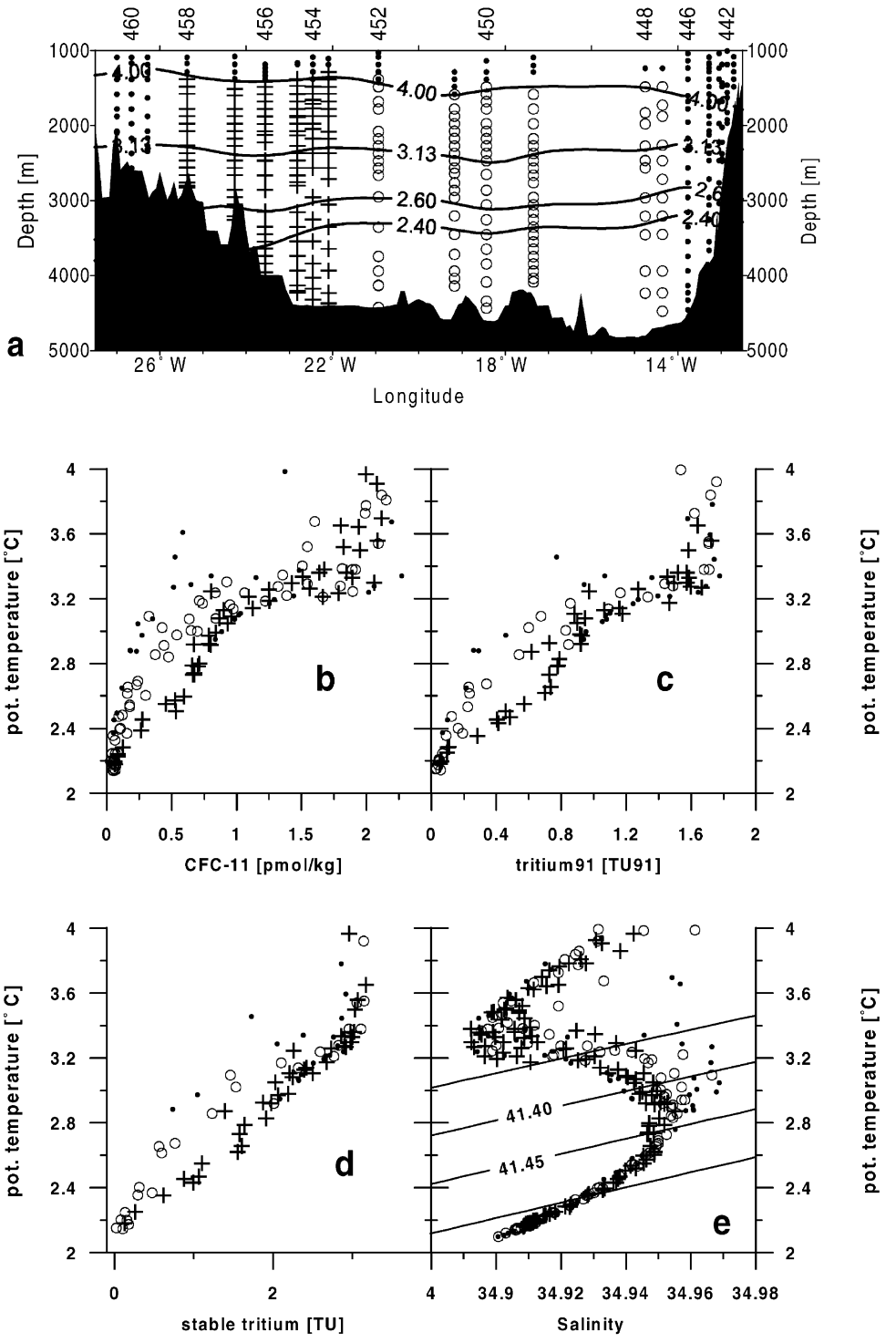
460
458
456
454
452
450
448
446
442
1000
2000
3000
4000
5000
Depth [m]
4.00
3.13
2.60
2.40
a
26° W
22° W
18° W
14° W
Longitude
b
c
pot. temperature [°C]
CFC-11 [pmol/kg]
tritium91 [TU91]
d
e
stable tritium [TU]
Salinity
41.40
41.45
34.9
34.92
34.94
34.96
34.98

(Fig. 4, ○). The temperature range corresponds to depths from 2500 to 3500 m (Fig. 4a). The higher tracer values indicate a recently ventilated water mass spreading into the eastern North Atlantic at densities below $\sigma_3 = 41.35$, corresponding approximately to $\sigma_\Theta = 27.8$. The newly ventilated Labrador Sea Water (LSW) is not that dense and Denmark Strait Overflow Water (DSOW) does not enter the eastern basin from the west to any significant extent. The enhanced tracer concentrations can therefore be assigned to the influence of Iceland Scotland Overflow Water (ISOW).

On the section A1 ISOW can be seen in all properties as a group of measurements with anomalously high values (Fig. 5, ×). In addition, measurements in the central Iceland Basin (IB) (Fig. 5, ▼) are influenced by ISOW as illustrated by CFC-11, tritium91 and stable tritium values, which are higher in the IB than the water at the same temperature in the Rockall Trough (Fig. 5, ○). The elevated values are found over a temperature range which clearly indicates that the increase is due to ISOW and not LSW. The difference is nearly invisible in the Θ–S diagram.

2.3. Method

For a quantitative analysis of the transport of deep water from the IB to the WEB the water with increased tracer values near the MAR is regarded as being an isopycnal two-component mixture. The two components considered are recirculated water originating from the eastern part of the WEB ($NEADW_{eWEB}$) and water from the Iceland Basin which is influenced by ISOW ($NEADW_{IB}$) (Fig. 6). The ISOW core itself is not considered as a source water. It can be seen in a section from A1 to the MAR just south of the GFZ realised in 1997 (*Meteor* cruise M 39/5, ▽ in Fig. 1, M. Rhein, pers. comm.) that it is not the core water itself that passes by the GFZ, but water with properties similar to the ones found in the Iceland basin adjacent to the core. The fractions of the two components cannot be deduced from Θ and S because the NEADW varieties do not differ enough compared to their variability for $2.4^\circ C < \Theta < 3.2^\circ C$ (Fig. 7).

The water masses do differ significantly in their tracer values (Fig. 4), and these are used to determine the fraction and transport time of $NEADW_{IB}$. The analysis is performed separately for each density interval of 0.01 for σ_3 between 41.35 and 41.52. Mean tracer values for the density levels are determined from the above-described data set. Using the assumption of a two-component mixture the tracer concentrations ($Tr_{wWEB}(1994)$) in the deep water mass observed near the MAR in 1994 are represented by the following equation:

$$\begin{aligned} &Tr_{wWEB}(1994) = x_{IB} \cdot Tr_{IB}(1994 - t_{IB}) + (1 - x_{IB}) \cdot Tr_{eWEB}(1994 - t_{eWEB}) \\ &\text{with} \quad x_{IB} + x_{eWEB} = 1 \quad \text{(mass conservation)} \end{aligned} \tag{2}$$

Fig. 4. Correlation diagrams of Θ–CFC-11 (b), Θ–tritium91 (c), Θ–stable tritium (d) and Θ–S diagram (e) for the deep part of the eastern North Atlantic ($\Theta < 4^\circ C$) on WHP section A2 in 1994 (*Meteor* 30/2). Stable tritium and tritium91 are derived from the measurements as explained in the text. Sampling locations and station numbers are shown in (a). Θ isolines have been added in (a) and isopycnals (spacing 0.05 in σ_3) in (e) to help with the identification of the corresponding depths and densities (σ_3) ($2.4 \Rightarrow 41.50$; $2.6 \Rightarrow 41.475$; $3.13 \Rightarrow 41.37$). The measurements near the MAR (+ , St. nos. 453–458) have higher tracer values for $2.4 < \Theta < 3.2^\circ C$ than those in the eastern part of the WEB (○, St. nos. 447–452). The measurements marked with circles are used to define $NEADW_{eWEB}$, the crosses for the definition of $NEADW_{wWEB}$.

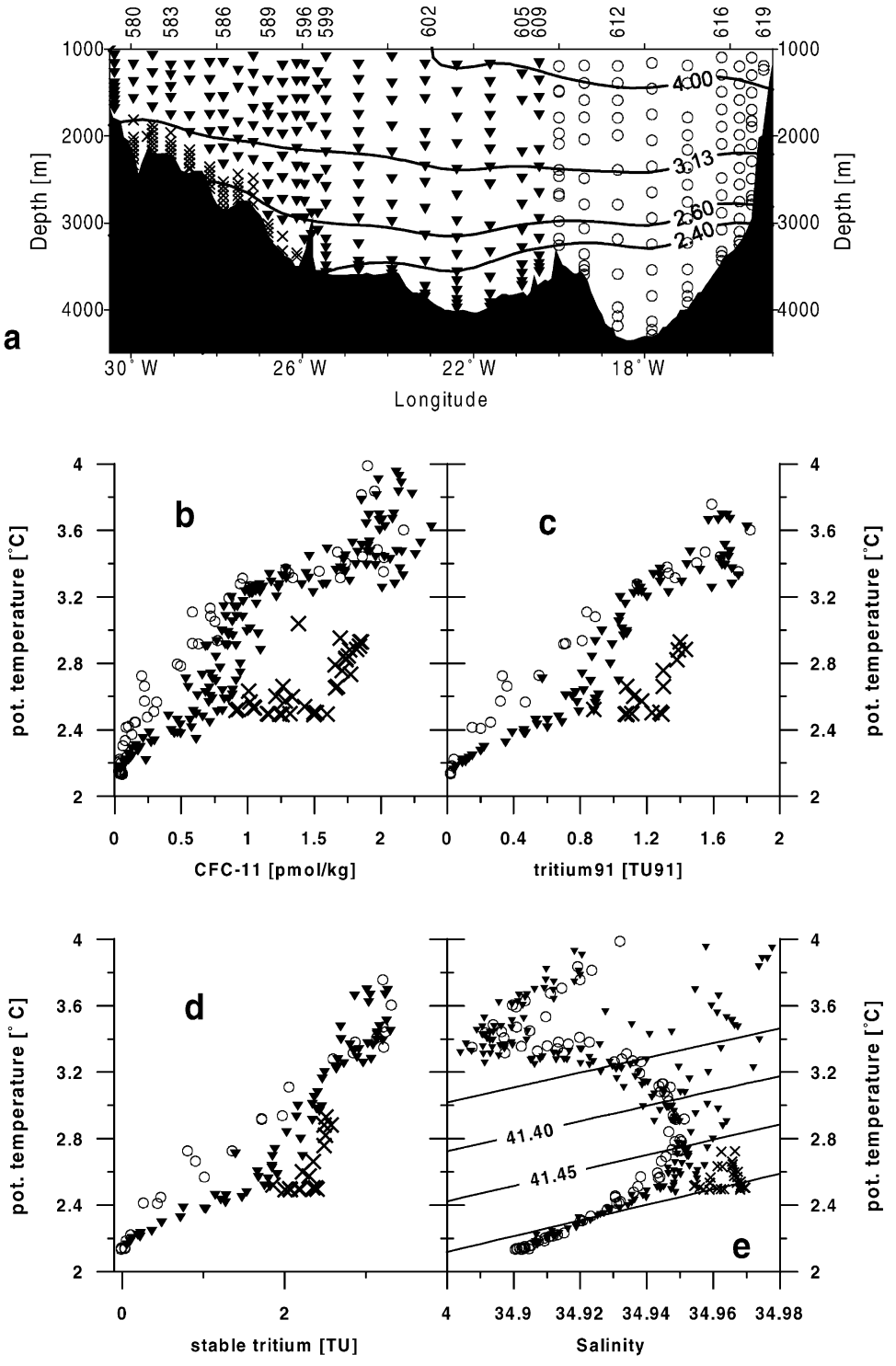
a
580
583
586
589
596
599
602
605
609
612
616
619
1000
2000
3000
4000
Depth [m]
4.00
3.13
2.60
2.40
30° W
26° W
22° W
18° W
Longitude
b
c
pot. temperature [°C]
CFC-11 [pmol/kg]
tritium91 [TU91]
d
e
stable tritium [TU]
Salinity
41.40
41.45
34.9
34.92
34.94
34.96
34.98

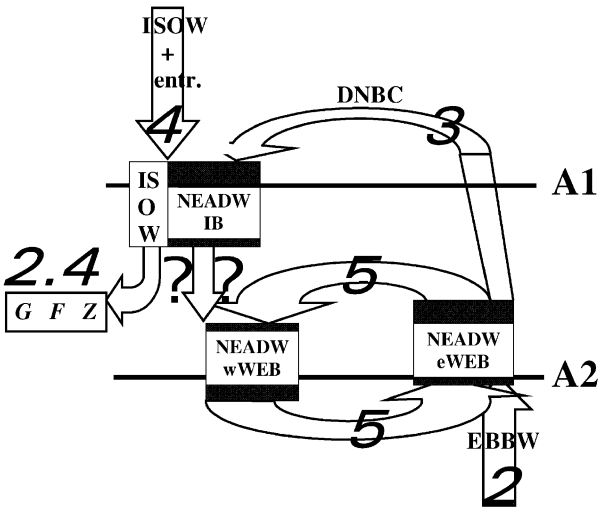

Fig. 6. Schematic flow pattern for the northeastern North Atlantic. The bold numbers are transports (in Sv) according to Schmitz and McCartney (1993), which do not account for any transport of deep water from the Iceland Basin to the Westeuropean Basin. At the GFZ the transport estimate of Saunders (1994; 2.4 Sv) is given.

The equations hold for all three tracers considered, i.e. CFC-11, tritium91 and stable tritium, and x_i denotes the fraction of each water mass present in the mixture. The tracer values of the two water masses have to be taken at the (unknown) time ($1994 - t_i$) when they left the place of their definition. These temporal offsets are the transport times that $\mathrm{NEADW_{IB}}$ (t_{IB}) and $\mathrm{NEADW_{eWEB}}$ (t_{eWEB}) respectively need to propagate from the place of their definition to the place where they are to be considered as part of the mixture. The same x and t values must fulfil Eq. (2) for CFC-11, tritium91 and stable tritium. This approach is similar to ratio dating in the assumption that the water is a two-component mixture, where both components have a certain age. It differs in the usage of a transport time rather than the time since leaving the surface and by considering tracers in both components. The latter adds the age of the second component as a third unknown.

In order to solve the 3 tracer equations (CFC-11, stable tritium and tritium91) for the 3 unknowns (t_{IB}, t_{eWEB}, x_{IB}) it is necessary to know or estimate the temporal evolution of the tracer values for $\mathrm{NEADW_{IB}}$ and $\mathrm{NEADW_{eWEB}}$. In ratio dating the temporal evolution of the tracer concentrations is commonly deduced from the input functions, which are sometimes modified to account for mixing or retardations of different water masses. The temporal evolution of the tracer concentrations in $\mathrm{NEADW_{IB}}$ and $\mathrm{NEADW_{eWEB}}$ are surely not directly proportional to the input

←

Fig. 5. Θ–tracer plots (b–d) and Θ–S diagram (e) for measurements in the deep eastern North Atlantic ($\Theta < 4^{\circ}\mathrm{C}$) on WHP A1 in 1991. Sampling locations and station numbers are shown in (a). Θ isolines have been added in (a) and isopycnals (spacing 0.05 in σ_3) in (e) to help with the identification of the corresponding depths and densities (σ_3). The measurements marked with (▼) define the $\mathrm{NEADW_{IB}}$. The purest form of ISOW ($\times$) is easily identified in all properties. Its influence on $\mathrm{NEADW_{IB}}$ can be seen by the increased tracer values of $\mathrm{NEADW_{IB}}$ compared to the measurements in the Rockall Trough (○).

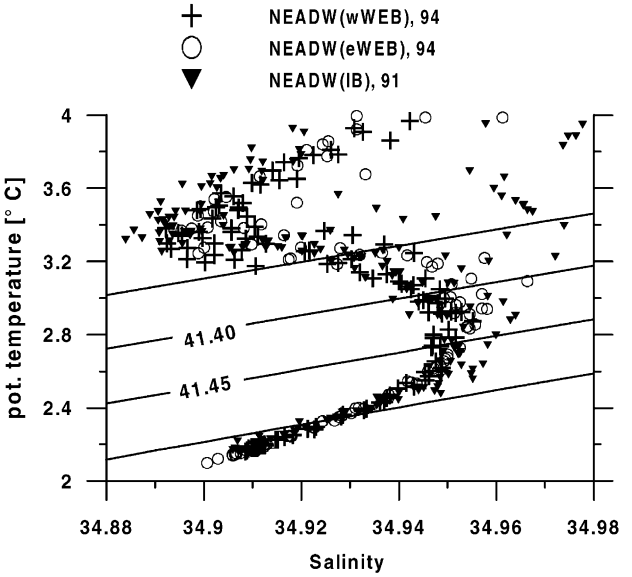

Fig. 7. Θ–S diagram for $NEADW_{IB}$ measurements (A1, 1991, ▼), $NEADW_{eWEB}$ (A2, 1994, ○) and $NEADW_{wWEB}$ (A2, 1994, +). The three varieties of NEADW are very similar and have a broad overlap.

function. The composition of these water masses from source water masses and their respective retardations are highly uncertain. The temporal evolution can alternatively be determined from preceding tracer measurements at the place where the source water masses are defined. This is in principle the best approach, but it is limited by the availability of data from the past. Nevertheless it is used for both water masses in this study.

The temporal evolution for $NEADW_{IB}$ is estimated from the two realisations of the A1 section, in 1991 and 1994. Averaged profiles are shown in Figs. 8a–c. The CFC-11 values of $NEADW_{wWEB}$ in 1994 are approximately as high as the 1991 $NEADW_{IB}$ values (Fig. 9). Since mixing with $NEADW_{eWEB}$ would lower the tracer concentrations, the $NEADW_{IB}$ does not need much longer than 3 yr for the way from the IB to the wWEB. A linear increase of the tracers is assumed between 1991 and 1994. The trends are quite different for the three tracers. Tritium91 (Fig. 8b) increases for $41.32 \leqslant \sigma_3 \leqslant 41.48$ by a factor of 1.26 ± 0.04 between 1991 and 1994. The input of tritium91 has been reasonably invariant between the mid-1960s and the 1990s (Fig. 2). Thus an increase of tritium91 suggests that the fraction of water formed after the beginning of the 1960s is increasing. In CFC-11 (Fig. 8a) a strong increase is found over the whole water column. The values in 1994 are 1.88 ± 0.07 times larger for $41.32 \leqslant \sigma_3 \leqslant 41.48$ than those in 1991. This corresponds to the steep increase in the CFC-11 input over time (Fig. 2). The fact that the CFC-11 values have increased by far more than the tritium91 values shows that the water found in 1994 is (as expected) on average formed later than that found in 1991. Stable tritium (Fig. 8c) increases strongly for high densities and only very little for lower densities. The input function of stable tritium strongly decreased after its maximum in the mid-1960s (Fig. 2). The behaviour of stable tritium compared to the other two tracers sheds light on the composition of the young part from different vintages. A minor increase of stable tritium with a stronger increase of tritium91 as noted for the lower densities can be

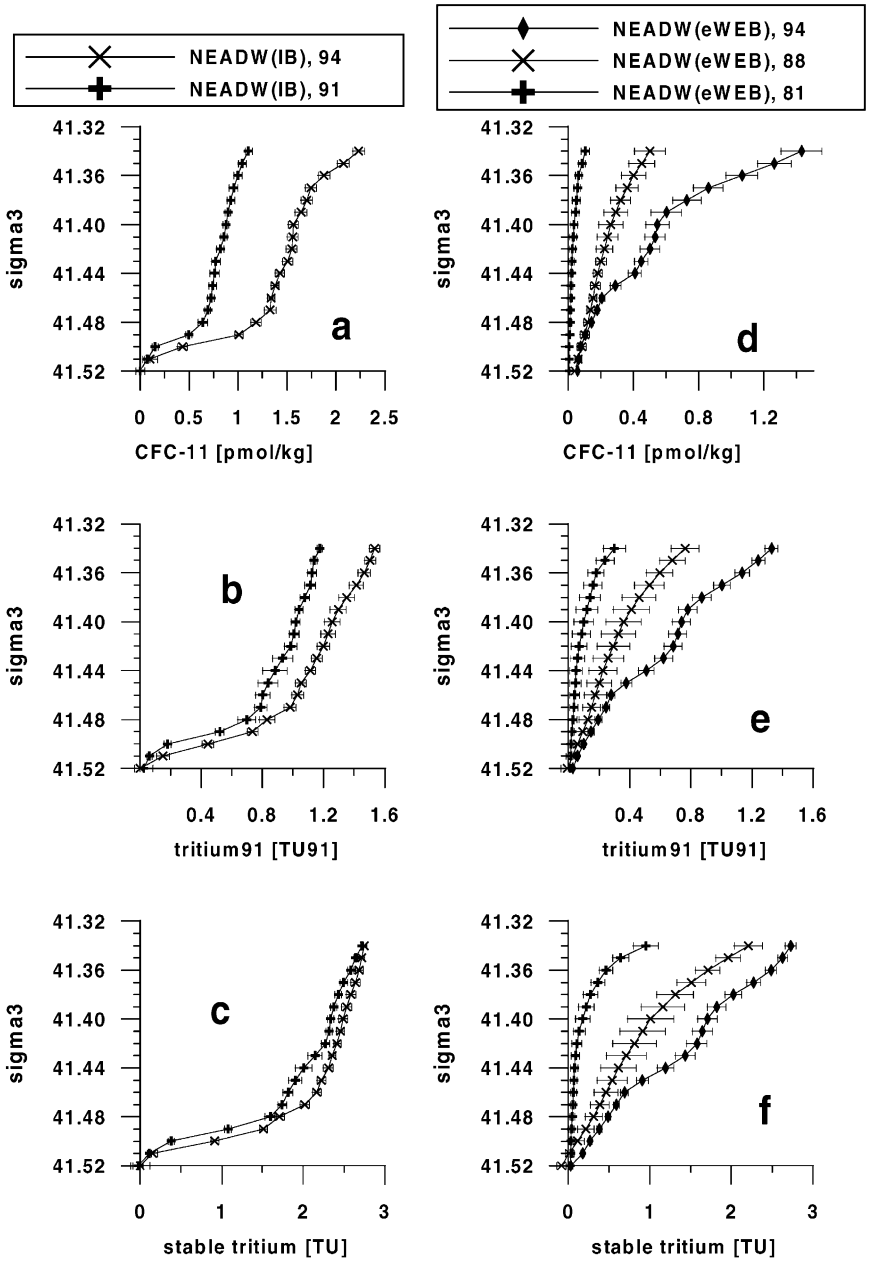

Fig. 8. Temporal evolution of the mean tracer profiles for $NEADW_{IB}$ (a–c) and $NEADW_{eWEB}$ (d–f). The error bars given are one standard deviation as determined in Section 3.2.

explained only by a decreasing amount of water from the earlier part of the high-tracer period (e.g. the 1960s) and a (stronger) increase in amounts of water from later periods (e.g. the 1980s).

The reconstruction of the past tracer concentrations worked well for the $NEADW_{IB}$, because it was possible to restrict the transport time to a maximum of about 3 yr. The tracer concentrations at

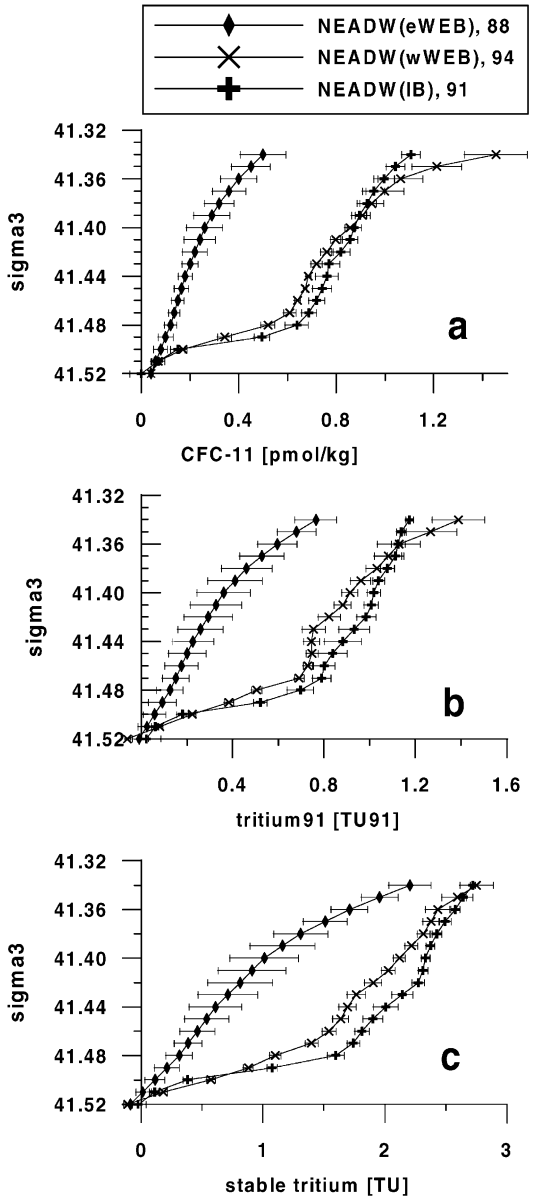

Fig. 9. Averaged profiles for CFC-11 (a), tritium91 (b) and stable tritium (c) for $NEADW_{wWEB}$ (1994, ×), $NEADW_{IB}$ (1991, +) and $NEADW_{eWEB}$ (1988, ♦). The profiles for $NEADW_{eWEB}$ and $NEADW_{IB}$ have a temporal offset to the $NEADW_{wWEB}$ profiles corresponding to their transport time resulting from this analysis. The error bars represent one standard deviation.

the beginning and end of the period in which the $NEADW_{IB}$ started at A1 are thus known. The situation is worse for the $NEADW_{eWEB}$, because there are no preceding tracer measurements on A2 and the transport time cannot be restricted in a similar way as for $NEADW_{IB}$. Data from other sections crossing A2 or being nearby are therefore used instead. This estimate is quite difficult to

achieve and uncertain because it is necessary to interpolate data, to use linear correlations between the tracers and to use data from further south. The results have a large uncertainty but they are nevertheless better than estimates based on the surface water history as shown in Section 4.

The temporal development of the $NEADW_{eWEB}$ tracer values is estimated from WHP A2 data from 1994 (M 30/2), A16N data from 1988 (*Oceanus* 202; Doney and Bullister, 1992; Doney and Jenkins, 1997), TTO tritium91 and stable tritium data from 1981 (Jenkins, 1988) and CFC-11 data from a cruise in the eastern North Atlantic carried out with the German research vessel *Meteor* in 1981 (M 56; Thiele, 1985). A16N and A2 intersect at 48°N, 20°W, which is in 1994 (A2) at the western edge of the $NEADW_{eWEB}$. In 1988 (A16N) the water at the intersection is obviously influenced by newly ventilated water, which is visible in CFC-11 values at 3000–3500 m that are higher than those in 1994. Therefore data from further south, where no such influence can be detected are used for the reconstruction of the tracer history of the $NEADW_{eWEB}$. This approach is limited by the requirement that LSW has to be the overlying watermass as it is on A2. Only station no. 49 (41°N) has low CFC values at 3000 m and an LSW maximum, but this is sampled very sparsely for CFC-11 and not at all for the other two tracers. The deeper part of the mean CFC-11 profile for 1988 (Fig. 8d, ×) is therefore constructed following the more southern profiles (nos. 49–57, corresponding to 41–37°N) and the shallower parts are oriented at the profiles showing a LSW maximum (nos. 33–49, corresponding to 49–41°N). The mean tritium91 and stable tritium profiles for 1988 (Figs. 8e and f, ×) are constructed from the CFC-11 profile using the quasi-linear relationship[2] between these two and CFC-11, which is found in the part of the water column with $\sigma_3 > 41.35$ whether it belongs to the more northern or the more southern profiles considered here (Fig. 10).

For 1981 the four TTO/NATS stations west of 20°W and north of 40°W (nos. 114–117) were used to determine the mean tritium91 and stable tritium profiles (Figs. 8e and f, +). CFCs have not been measured in the frame work of TTO/NATS, and the only available CFC-11 data for this year are from a cruise with the German research vessel *Meteor* (Thiele, 1985). But there are only two stations north of 40°N, and the CFC-11 profiles only reach to depths of 1500 m. The task now is to estimate the tracer profile for depths below 2500 m as sensibly as possible from these data. We rely again on the existence of a quasi-linear relationship between tritium91 and CFC-11, which has been used for the construction of the A16N profiles and is found to exist for the A2 data as well. The ratio valid for the deep water is estimated in two ways: at first from the measurements at depth between 1000 and 1500 m and then from the extrapolated change of the ratio between 1988 and 1994. The depth range 1000–1500 m is the transition zone between the LSW and the intermediate waters and has nearly constant CFC-11 and tritium91 values in the data sets of the three years (1994, 1988, 1981). For M30/2 and A16N the slope of a straight line through the origin fitting the CFC-11 and tritium91 data in the deep water (0.78 and 0.69, respectively) can be coarsely estimated from the ratio of CFC-11 and tritium91 in depths of 1000–1500 m (1.11 and 0.79, respectively). The CFC-11/tritium91 ratio for 1981 is therefore determined for the water between 1000 and 1500 m (five M56 measurements for CFC-11 with 0.37 ± 0.05 pmol/kg, 14 TTO measurements for

[2] Tritium91 (TU91) = 1.65 [TU91/(pmol/kg)]CFC-11 (pmol/kg) + 0.07 (TU91), correlation coefficient: 0.9504; stable tritium (TU) = 4.86 [TU/(pmol/kg)]CFC-11 (pmol/kg) − 0.26 (TU), correlation coefficient: 0.966.

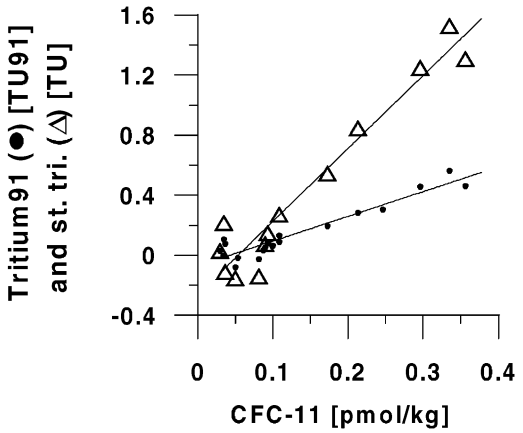

Fig. 10. Stable tritium (△) and tritium91 (●) plotted versus CFC-11. The linear regression lines of both tracers on CFC-11 are shown as well. For $\sigma_3 > 41.35$ on A16N (st. nos 33–57).

tritium91 with 1.07 ± 0.18 TU91, resulting ratio: 0.346). The CFC-11 profile is then derived by multiplying the tritium91 profile by the factor 0.346. This ratio is very low compared to the ratios in 1994 (0.78) and 1988 (0.69). Such a steep decrease does not fit the temporal change of the ratio. A linear extrapolation of the decrease of the ratio with time leads to a ratio of 0.59 for 1981. This corresponds to the linear change of the ratio in the surface water which was found for a long period of time (Fig. 2). A CFC-11 profile derived from the tritium91 profile by multiplying with a factor of 0.59 was therefore used in the final run. The temporal evolution of the tracer concentrations in $NEADW_{eWEB}$ between the cruises is then constructed from linear interpolations between the calculated concentrations for the observation times and a state with no tracers assumed for 1971.

The averaged tracer profiles for the $NEADW_{wWEB}$ (Fig. 9) are defined from the WHP A2 (1994) data near the MAR (+ in Fig. 4). These are the concentrations that have to be explained by the mixing analysis. They are shown together with one $NEADW_{eWEB}$ profile (1988) and one $NEADW_{IB}$ profile (1991). The profiles are defined for $41.34 < \sigma_3 < 41.52$. However, a significant difference between the tracers of $NEADW_{eWEB}$ and $NEADW_{wWEB}$ is found in 1994 only for $41.37 < \sigma_3 < 41.50$. The further analysis is therefore restricted to this density range.

The transport time of $NEADW_{eWEB}$ is not determined directly from the set of the three equations. Instead the calculations are carried out varying this parameter from 0 to 23 yr. Since the tracer values for $NEADW_{eWEB}$ are assumed to be zero in 1971 (23 yr spreading time), longer spreading times cannot be distinguished from the run with $t_{NEADW(eWEB)} = 23$ yr.

3. Results

x_{IB} and t_{IB} are determined from the optimal least squares solution of the three tracer equations for the given values of t_{eWEB}. This is done separately for every density interval of 0.01 for σ_3 between

41.37 and 41.51 by minimising the root mean square (e) of the weighted tracer deviations (d) between the measured values ($\mathrm{Tr}_{\mathrm{meas}}$) and those resulting from the analysis ($\mathrm{Tr}(x_{\mathrm{IB}},\ t_{\mathrm{IB}})$):

$$e = \sqrt{d \cdot d'/3}, \tag{3a}$$

where

$$d = \left[\begin{pmatrix} \text{CFC-11} \\ {}^{3}\text{H91} \\ \text{st.tri.} \end{pmatrix}_{\text{meas}} - \begin{pmatrix} \text{CFC-11}(x_{\mathrm{IB}}, t_{\mathrm{IB}}) \\ {}^{3}\text{H91}(x_{\mathrm{IB}}, t_{\mathrm{IB}}) \\ \text{st.tri.}(x_{\mathrm{IB}}, t_{\mathrm{IB}}) \end{pmatrix} \right] \cdot W \tag{3b}$$

with

$$W = \begin{pmatrix} 1/\text{mean } (\sigma_{\mathrm{CFC}}) & 0 & 0 \\ 0 & 1/\text{mean } (\sigma_{^{3}\mathrm{H91}}) & 0 \\ 0 & 0 & 1/\text{mean } (\sigma_{\mathrm{st.tri.}}) \end{pmatrix}.$$

The elements of the diagonal weighting matrix (W) are the reciprocal values of the mean uncertainties of the respective tracer at the considered density in the contributing water masses. The elements of d therefore represent the deviation of the respective tracer measured in units of its uncertainty. $d \cdot d'$ (with d' being the transpose of d) is the sum of the squared deviations, which is divided by the number of contributing deviations (i.e. three). In order to get an easily understandable measure of the deviation e the square root of this term is taken. e defined as above is the root mean square of the tracer deviations measured in their respective uncertainties. This deviation has to be less than one if the mixing assumptions and error estimates are correct. Unfortunately a value below one does not automatically imply that all assumptions are correct.

The resulting profiles of x_{IB} and t_{IB} for $t_{\mathrm{eWEB}} = 3$, 6 and 23 yr are shown as examples in Fig. 11. The fraction of x_{IB} (Fig. 11a) and the transport time t_{IB} (Fig. 11b) do not change considerably in the density range considered. The fraction is slightly decreasing and the transport time is slightly increasing with density. Combined with an approximate distance of 650 km these transport times yield effective spreading velocities of about 0.8 cm/s. The quotient of the two quantities ($\tau = x_{\mathrm{IB}}/t_{\mathrm{IB}}$, Fig 11c) is a measure for the transport of $\mathrm{NEADW_{IB}}$ (Eq. (4)). τ has less scatter and uncertainty and is therefore a more stable result than the fractions and transport times themselves. This emerges because higher fractions combined with shorter transport times or vice versa result in similar tracer contributions of the $\mathrm{NEADW_{IB}}$. τ decreases more steadily from lower to higher densities indicating a decreasing $\mathrm{NEADW_{IB}}$ flux density. The steady behaviour of τ stops for $\sigma_3 > 41.48$. The fraction and transport time for $\sigma_3 = 41.48$ are noticeably smaller than all others, which is rather improbable. Therefore only results from $\sigma_3 < 41.475$ are considered to be reliable. The measure of the deviation is below or nearly equal to 1 (maximum of 1.06) for $41.37 \leqslant \sigma_3 \leqslant 41.47$.

The results of all runs are very similar except those with $t_{\mathrm{eWEB}} < 3$ yr, which have considerably lower values of τ for $\sigma_3 < 41.45$. A value of $t_{\mathrm{eWEB}} = 10$ yr corresponds to an effective spreading velocity of 0.32 cm/s for a supposed length of the recirculation path of 1000 km (corresponding to a semicircle with a diameter of about 8° longitude extending about 3° to the north). A transport time of less than 3 yr implies thus an effective spreading velocity of 1 cm/s or more. This would be faster than the spreading of the $\mathrm{NEADW_{IB}}$, and even the spreading velocities in the Deep Western

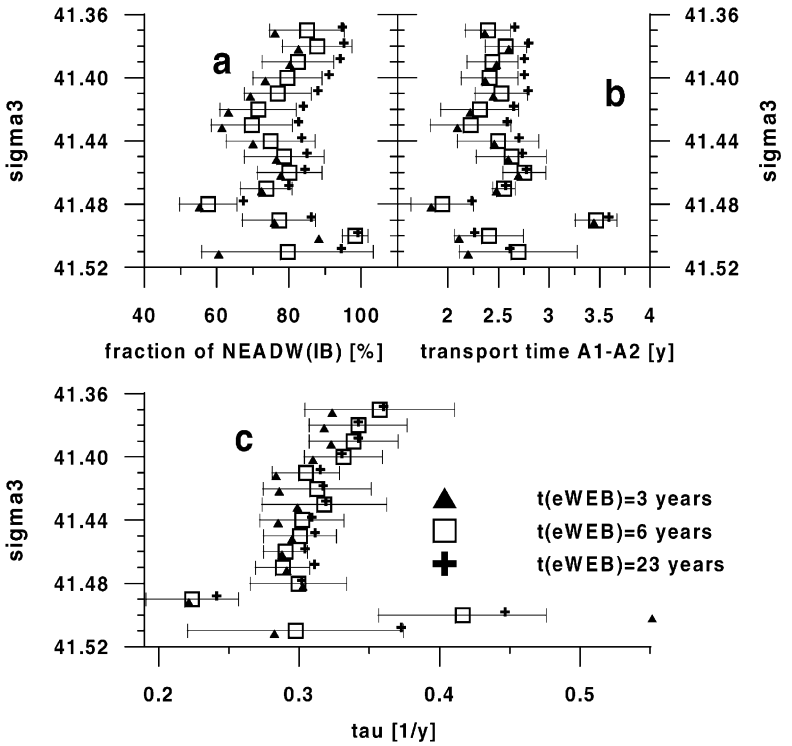

Fig. 11. Profiles of the fraction (a) and transport time (b) of $NEADW_{IB}$ for $t_{eWEB} = 3$ (▲), 6 (□) and 23 yr (+). (c) The quotient of the fraction and the transport time (τ). This is a measure of the flow and is a more stable result of the analysis (see text). The error bars represent one standard deviation and belong to the run with $t_{eWEB} = 6$ yr.

Boundary Current reported in Smethie et al. (2000) do not exceed 1–2 cm/s. The recirculating $NEADW_{eWEB}$ is not part of a current system of similar strength, and spreading velocities exceeding 1 cm/s are therefore assumed to be unrealistic. The results of runs with $t_{eWEB} < 3$ yr are therefore neglected for the further analysis. The average of the deviation e over all density levels reaches a minimum at $t_{eWEB} = 6$ yr (Table 2). The minima for individual density levels are between 5 and 8 yr. They show a slight but strongly scattered increase towards higher densities. The minima of e are a further reason to assume transport times of at least 3 yr rather than a spreading velocity of more than 1 cm/s.

3.1. Deep water transport to the Westeuropean Basin

The calculated profiles of the mean effective transport time and the mean fraction of $NEADW_{IB}$ shall now be used to calculate an effective southward transport of deep water from the Iceland Basin to the Westeuropean Basin. The distance between A1 and A2 (d) is divided by the transport time (t_{IB}) to yield the effective spreading velocity (v). This velocity is smaller than the actual velocity, because it only considers the displacement over a period of time and does not account for any deviation from the direct way (Jenkins, 1988). v has to be multiplied by the area (A) occupied by the

Table 2
Resulting transports of $NEADW_{IB}$ in Sv (first row) integrated in the range $41.37 < \sigma_3 < 41.475$ for different values of t_{eWEB}. The uncertainty given is one standard deviation, where uncertainties in the distance A1–A2 (7.7%), the area (10.7%) and the transport parameter τ (second row) are considered. The third row gives the average of the root mean square of the tracer deviations over all considered density levels

t_{eWEB}	3 yr	6 yr	9 yr	13 yr	18 yr	23 yr
Transport (SV)	1.58 ± 0.27	1.66 ± 0.27	1.67 ± 0.25	1.69 ± 0.25	1.70 ± 0.25	1.70 ± 0.25
σ_τ (Sv)	0.17	0.16	0.11	0.10	0.10	0.10
Mean e	0.359	0.303	0.353	0.495	0.601	0.754

flow to calculate a transport. The distance and the area are attributes of the individual measurements (d_i, A_i), and therefore we assign values and uncertainties of the transport time ($t_{IB,i}$), the fraction of $NEADW_{IB}$ ($x_{IB,i}$) and the transport parameter ($\tau_i = x_{IB}/t_{IB}$) to every measurement via its density. The transport vA must be multiplied by the fraction of $NEADW_{IB}$ (x_{IB}), because we are only interested in the flow of $NEADW_{IB}$ across the section and this only accounts for the fraction of the area given by x_{IB}. The transport of $NEADW_{IB}$ is finally the sum of the transports calculated for individual measurements:

$$T = \sum_i A_i v_i x_{IB,i} = \sum_i A_i (d_i/t_{IB,i}) x_{IB,i} = \sum_i A_i d_i \tau_i \tag{4}$$

with i running over measurements belonging to $NEADW_{wWEB}$.

The effective spreading is assumed to be southward, and thus only the meridional distances between the measurements on A2 and A1 are used for d_i and only the area perpendicular to the effective spreading direction has to be considered. The area A_i represented by every measurement is therefore calculated by multiplying half of the zonal distance to the neighbouring stations and half of the vertical distance to the samples above and below. All measurements with $41.37 < \sigma_3 < 41.475$ for stations where elevated tracer values were found (St. nos. 453–458) have been used for the calculation of the transport. For these measurements Θ ranges between 2.60 and 3.13°C (Fig. 4a).

The resulting transports in the σ_3 interval 41.37–41.475 for selected values of t_{eWEB} are given in Table 2. They range between 1.58 and 1.70 Sv, which shows that the result is not very sensitive to the choice of t_{eWEB}.

The transport calculation was restricted to $41.37 < \sigma_3 < 41.475$, because the results were unstable for higher densities or no tracer difference existed between the eastern and western part of the WEB in 1994. However, this does not mean that there is no transport of water from the IB to the WEB on these levels. Even though the results were unstable, it is still obvious that a tracer difference exists for $41.475 < \sigma_3 < 41.50$ (corresponding to $2.4°C < \Theta < 2.6°C$, Fig. 4a). For the comparison with other studies, which frequently use $\sigma_\Theta > 27.8$ ($41.35 < \sigma_3$) for the definition of deep water, the transport is estimated in this density range as well (see Fig. 4a for data location: + below the $\Theta = 3.13°C$ isoline and 6 measurements above). The assumption that part of the $NEADW_{IB}$ transport is achieved in higher density levels is supported by the fact that the currents measured with or adjusted by (L)ADCPs are very frequently found to have the same direction

throughout the whole water column (for the Iceland Basin see e.g. Bersch, 1994). The transport is estimated for the density levels, for which it could not be taken from the above analysis in different ways in order to get an idea of the order of magnitude the transport could have in these density levels. At first the averaged transport per unit area is calculated and multiplied by the area covered by measurements with $\sigma_\Theta > 27.8$. This results in a transport of 3.5 Sv of $NEADW_{IB}$ from the IB to the WEB. 2.4 Sv results for $41.37 < \sigma_3 < 41.50$. The second approach is based on a linear extrapolation of τ on σ_3. Combining the estimates of τ from the linear regression with the station data as described above results in a transport of 3.2 Sv for $\sigma_\Theta > 27.8$ and 2.3 Sv for $41.37 < \sigma_3 < 41.50$. The third approach is based on the assumption that there is no $NEADW_{IB}$ at $\sigma_3 = 41.51$, where no tracer difference is found. The fraction of $NEADW_{IB}$ is therefore taken to be zero there, and a linear decrease between $\sigma_3 = 41.47$ and 41.51 is assumed. τ is calculated from these fractions with a constant transport time $t_{NEADW(IB)}$ of 2.5 yr. This leads to a transport of 2.4 Sv for $\sigma_\Theta > 27.8$, but densities exceeding $\sigma_3 = 41.51$ do not contribute because of the above assumption on the composition of the water.

3.2. Uncertainty of the transport

We will now discuss the uncertainty of the above presented transport estimate. The uncertainty of the transport calculated for $41.37 < \sigma_3 < 41.475$ is caused by uncertainties of τ, of the distance d between A1 and A2 and of the area A (Eq. (4)). The uncertainties of τ are caused by variations of the tracers on the density levels. These variations include natural variability as well as the uncertainties due to measurement precision. The variations of tracers on the density levels are used to deduce the uncertainties of the mean profiles, which in turn yield the uncertainty of τ. The mean profiles are determined by calculating a weighted mean of measurements in the vicinity of the considered σ_3 value (an example is shown in Fig. 12). The standard deviation for an individual measurement (dashed line in Fig. 12) was determined as a weighted average of the deviations of the considered measurements from the mean profile. The standard deviation of the mean (dotted line in Fig. 12) is calculated by dividing the standard variation for the individual measurements by the square root of the number of elements minus one effectively contributing to the value. The effective contributions are determined by the weight with which the measurements contributed to the calculation of the mean value. This procedure has been applied to the densely sampled profiles of 1991 and 1994. For the $NEADW_{eWEB}$ determined from A16N (1988) and TTO (1981) data it was impossible to proceed in the same way. For the CFC-11 data in 1988 the relative uncertainty for an individual measurement is estimated to be the same as the uncertainty for an individual measurement in 1994, which agrees well with the data distribution. But because there are very few measurements, the uncertainty of the mean profile is taken to be the same as the uncertainty for an individual measurement without dividing by the square root of the contributing elements (minus 1). The relative errors are therefore about twice as large for 1988 as for 1994. The tritium91 and stable tritium data were derived from the linear regression of these two tracers on CFC-11. Because this procedure carries additional uncertainties the relative uncertainties for individual measurements taken from 1994 have been doubled to obtain an estimate for 1988. The relative uncertainties are then about four times as high in 1988 as in 1994. For the 1981 data the quadrupled relative uncertainties have been chosen for all three tracers. The uncertainties estimated in this way are compatible with the sparse data that was used for the determination of the profiles. The calculation

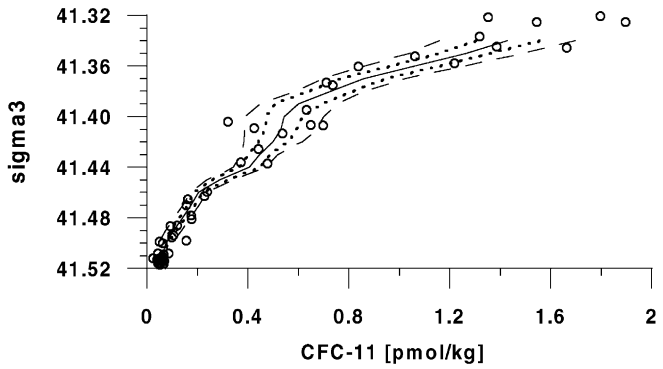

Fig. 12. Averaged CFC-11 profile (solid line) and measurements (○) for $NEADW_{eWEB}$ in 1994. The space between the dashed lines covers one standard deviation for an individual measurement. The dotted line shows one standard deviation of the mean. Their determination is described in Section 3.2.

of the transport has been carried out 500 times under random variations of all tracer values to propagate the uncertainty of the mean profiles to an uncertainty of τ. Random amounts of tracers in the magnitude determined as standard variation of the mean profiles have been added or subtracted independently to the mean tracer value in each run. The standard deviations of the transports caused by the uncertainty of τ (σ_τ) resulting from these 500 calculations are given in Table 2.

The meridional distance between the measurements on A2 and A1 varies between 600 and 750 km depending on the longitude. The respective distances for each longitude have been used to calculate the transport even though we cannot know for sure from which place on A1 the water seen on A2 has actually started. The uncertainty due to the distance is therefore taken from the calculation of the mean meridional distance between A1 and A2 (645 ± 50 km or a relative uncertainty of 7.7%). Since the transport is calculated from an effective southward spreading velocity it does not matter if the water moves as well east–west or is moving back and forth north–south on its way.

The main uncertainty of the area is due to the assumption that the boundary of the $NEADW_{wWEB}$ to the neighbouring water masses is in the middle, between the stations that fall into the $NEADW_{wWEB}$ cluster and those that are outside. The area used in the $NEADW_{IB}$ transport calculations would increase by 10.7% if the boundaries of the $NEADW_{wWEB}$ were just next to the first stations outside. The area would decrease by this amount if the boundaries were just next to the last stations inside the $NEADW_{IB}$. Therefore an uncertainty of 10.7% is assigned to the area. The total uncertainty results from error propagation of the uncertainties of the area, the distance and τ. This uncertainty of the transport is given in the first row of Table 2.

A last uncertainty arises from the assumption that the temporal trend in the tracers is linear. This is the best approximation in the absence of further knowledge, but may be an unreliable assumption. Because the calculated transport time for $NEADW_{IB}$ is about $2\frac{1}{2}$ yr the water found on A2 in 1994 is formed in about 1991 and for this time the concentrations are well defined by the realisation of A1 in 1991. The uncertainty caused by the assumption of a linear trend is therefore of minor importance.

The temporal trend in the tracers of the $NEADW_{eWEB}$ is assumed to be linear as well and has additionally been deduced from sparse data. A much bigger uncertainty has been assumed for the profiles in 1988 and 1981 to account for the sparseness of the data. But the $NEADW_{IB}$ has higher tracer values than the $NEADW_{eWEB}$ and its fraction (x_{IB}) amounts to more than 75% of the mixture and thus it contributes a large proportion of the tracers. Uncertainties in the temporal evolution of the $NEADW_{eWEB}$ therefore only have a minor influence on the results. This is emphasised by the insensitivity of the results to changes of t_{eWEB} (Table 2 and Fig. 11).

The uncertainty belonging to $NEADW_{wWEB}$ measurements with densities exceeding $\sigma_\Theta = 27.8$ and not belonging to the density range $41.37 < \sigma_3 < 41.475$ cannot be calculated in a formal way as presented above. This uncertainty depends rather on the assumptions used for the extrapolation than on uncertainties of measurements and parameters contributing to the calculation. It can therefore only be said to lie in the range between 2.4 and 3.5 Sv, with these two values resulting from extrapolation methods which tend to underestimate and overestimate the transport, respectively.

4. Discussion

The results of this study are based on the assumption that $NEADW_{wWEB}$ is an isopycnal two-component mixture of $NEADW_{eWEB}$ and $NEADW_{IB}$. Diapycnal mixing between these two water masses is not expected to be important, because there are no considerable horizontal density gradients between the two water masses. A third water mass that exists in the same density range is the ISOW core. This purest form of ISOW on A1 is found at the eastern flank of the Reykjanes Ridge. Strong horizontal density gradients are found in this region allowing for diapycnal mixing. The salinity of this water mass is considerably higher than that of the water considered here. A significant contribution of the ISOW core water would lead to an observable shift towards higher salinities. The absence of a significant salinity shift means that a direct influence of water from the ISOW core is negligible.

But it can be concluded from tracers that $NEADW_{IB}$ itself must be a mixture of an ISOW variety with $NEADW_{eWEB}$ which is found further east in the Rockall Trough. The profiles on A1 in the Iceland Basin and the profiles on A1 in the Rockall Trough are very similar in the transition zone to the LSW that forms the upper part of the profiles in Fig. 5. This proves that the high tracer values of $NEADW_{IB}$ are not caused by vertical mixing. They are due to the influence of ISOW and its entrainment. However, only a small influence of ISOW on $NEADW_{IB}$ is seen in salinity (Fig. 5e). It is only slightly more saline than $NEADW_{eWEB}$. The influence of ISOW is obvious in tritium91 and CFC-11. The ISOW in $NEADW_{IB}$ must therefore have a different composition to the ISOW found at the Reykjanes Ridge. The admixed ISOW variety must be high in tracers, but must not have as high salinities as the ISOW found at the Reykjanes Ridge. A larger amount of entrained LSW in this variety could explain a small salinity effect combined with a strong tracer effect. The importance of LSW as part of the entrainment to the ISOW has been found for example by Harvey and Theodorou (1986) and van Aken and de Boer (1995). LSW is probably found with larger fractions in the water outside the core because the core itself is more protected against mixing with LSW by this 'coating'. This does not mean that only LSW is entrained into the cold outflow of the Norwegian Sea in the formation process of $NEADW_{IB}$, but it is probably a more important part of the mixture than in the formation process of the ISOW core itself.

For the transport calculation the effective spreading direction was assumed to be southward. If the direction of the mean transport deviates from this direction by the angle α a longer pathway (factor $1/\cos\alpha$) would result and thus a higher effective spreading velocity. The transport would not change, however, because the area would no longer be at right angles to the transport. The area would have to be multiplied with the factor $\cos\alpha$, which just cancels out the effect of the increased pathway. This is true as long as the volume flushed by the water is constant. If a bigger volume is flushed for example by a mean flow that moves eastward at first and southward thereafter a higher transport would result.

The measured development over time has been used to estimate the temporal evolution of the tracer concentrations of $NEADW_{IB}$ and $NEADW_{eWEB}$ in this study. As a consequence all effects like undersaturation during the formation process or the complex mixing processes involved in the formation of the water masses did not have to be dealt with explicitly. The big advantage of this method — even if only sparse data are available — compared to estimates based on input functions is demonstrated by the example of the temporal evolution of tritium91 on $\sigma_3 = 41.42$ for $NEADW_{eWEB}$ (Fig. 13). One way to estimate a hypothetical temporal evolution of tritium91 from the input function could be ratio dating based on the 1994 data only. In a first step the age (t, e.g. 20.4 yr) and fraction (x, e.g. 34%) of the young component are calculated from the 1994 (A2) $NEADW_{eWEB}$ data. To calculate a tracer value at an earlier time (T, e.g. 1988) it is then assumed that the fraction and age of the young component are the same at all times. The tracer value at T results from multiplying the amount of young fraction (x) by the surface water tracer value (Fig. 2) of the year $T - t$ (1967.6 = 1988 − 20.4 in the example). The temporal evolutions of tritium91 estimated in such a way from CFC-11/tritium91 ratio dating and stable tritium/tritium91 ratio dating are given as solid lines in Fig. 13. The two differ from one another in the calculated ages by

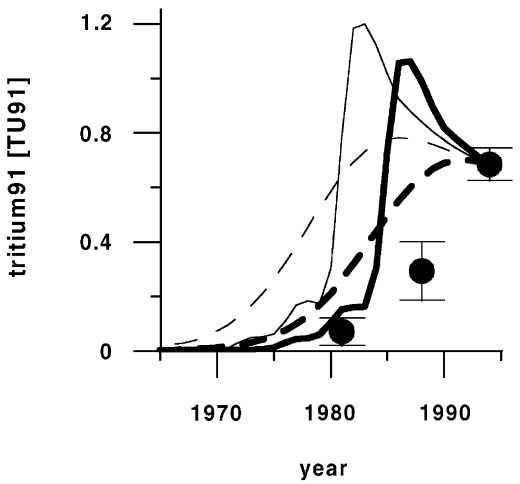

Fig. 13. Temporal evolution of tritium91 on $\sigma_3 = 41.42$. Shown are estimates from stable tritium/tritium91 ratio dating (fine lines) and CFC-11/tritium91 ratio dating (bold lines). The solid lines are estimates from conventional ratio dating; the dashed lines are estimates from ratio dating based on low-pass filtered ($\sigma = 5$ yr) surface water histories. The solid circles give the tritium91 values for this water in 1994 (M30/2), 1988 (A16N) and 1981 (TTO). The error bars correspond to one standard deviation.

about four years, which causes a kind of offset between the two estimated temporal evolutions of tritium91. But both temporal evolutions resulting from the ratio dating are bad estimates of the real tritium91 values in 1988 and 1981, even if these have a still bigger uncertainty than assumed.

The above-discussed calculation method was based on traditional ratio dating, which implies that the water is looked upon as a mixture of old water without any tracers and a young component which has the tracer signature of a particular year. This is unrealistic since any water sample will be a mixture of waters of a broad spectrum of ages. In a more realistic approach the temporal evolution of tritium91 has therefore been estimated from ratio dating based on modified input functions which have been convoluted with gaussian distributions with a halfwidth of 5 yr (dashed lines in Fig. 13). The low-pass filtered versions of the input functions are more realistic approximations to the real formation of a water mass, because they allow for water from different years to contribute to the mixture. However, all four estimates of the tritium91 history of the $NEADW_{eWEB}$ differ significantly from one another and none of them is able to represent the measurements.

The biggest problem in any of the four estimations above is the assumption that the fractions remain unchanged for the whole time. The young fraction accounts for water that is formed from the 1960s onwards. In a steady-state situation the fraction of water that is younger than a certain age is constant. The young fraction calculated for 1994 accounts for water of ages up to about 34 yr. The correct young fraction (water formed in and after the 1960s) for ratio dating in 1988 would be the one of 1994 reduced by the part that accounts for water with an age between 28 and 34 years, because water with this age is formed before the 1960s in 1988. Since the distribution of the water among the different ages is unknown, there is no way to correct for this. The problems described here for tritium91 are less pronounced for CFC-11 but even larger for stable tritium due to the different temporal evolutions (Fig. 2). Going backwards along the input function therefore leads to moderately rising values of tritium91, strongly rising stable tritium and decreasing values of CFC-11; meanwhile the tracer concentrations are decreasing in the data for all three tracers.

5. Conclusion

Transport values have been calculated in this study varying the transport time from the eastern to the western WEB (t_{eWEB}) between 0 and 23 yr. For transport times $t_{eWEB} < 3$ yr the resulting effective spreading velocity describing the recirculation is higher than 1 cm/s, even exceeding the effective spreading velocity of $NEADW_{IB}$. Such velocities are unrealistically high and the corresponding transports have therefore been rejected. The best fit to the measurements was reached for $t_{eWEB} = 6$ yr, but all other results are very similar to this one. The high fractions of $NEADW_{IB}$ indicate that there is only a weak recirculation of $NEADW_{eWEB}$ directly to the western WEB. The results suggest that the $NEADW_{eWEB}$ flows to the north where it is mixed with ISOW and its entrainments. This mixture forms the water that is found in the central Iceland Basin ($NEADW_{IB}$). A part of this mixture is then transported southward to the WEB. An average transport of $NEADW_{IB}$ from the Iceland Basin to the Westeuropean Basin of 1.63 ± 0.32 Sv results from the six runs with varying transport times and their uncertainties given in Table 2 for $41.37 < \sigma_3 < 41.475$.

The increased tracer values near the MAR on the WHP A2 section and the transport estimate of at least 1.63 ± 0.32 Sv $NEADW_{IB}$ are clear evidence that not all ISOW leaves the eastern North Atlantic through the GFZ. A considerable part of the ISOW contributes to the deep water of the Iceland Basin and partially propagates from there to the WEB. The discrepancy in the transport through the GFZ between the results of a mooring array in the GFZ (2.4 Sv; Saunders, 1994) and the water supposed to form the Deep Northern Boundary Current and to flow through the GFZ (6.6 Sv + warm entrainment (McCartney, 1992), 6.7 Sv (van Aken and Becker, 1996), 7 Sv (Schmitz and McCartney, 1993), 9 Sv (Bersch, 1995)) is about 5 Sv. We have shown that at least 1.63 ± 0.32 Sv of the missing transport of deep water continues to flow southward and reaches the WEB instead of escaping to the western NA. The above-mentioned studies mostly refer to water with $\sigma_\Theta > 27.8$ while our estimates are for a smaller density range. Extending our transport estimates to this density range increases the deep water transport remaining in the eastern basin even to 2.4–3.5 Sv. This pathway therefore accounts for a considerable part of the disagreements on the GFZ transport mentioned above.

Acknowledgements

We would like to thank the captains, the crews and the scientists of the cruises from which data were used in this study. The CFC-11 data of the cruise *Meteor* 30/3 and 39/5 are courtesy of Monika Rhein; the A16N CFC-11 data were provided by John Bullister, the A16N and TTO ^{3}He and tritium data by Bill Jenkins. We would like to thank them for their co-operation. Alison Bateman was a great help in improving the English of this article, Birgit Klein supported the work by valuable discussions as did the reviewers with helpful comments. The data acquisition and interpretation were supported by the BMBF WOCE programme under grant nos. 03 F 0538 A, 03 F 0121 A and 03 F 0157 A and by the Deutsche Forschungsgemeinschaft under grant nos. Ro 318/46 and Ba 1303/4.

References

Bayer, R., Schlosser, P., Bönisch, G., Rupp, H., Zaucker, F., Zimmek, G., 1989. Performance and Blank Components of a Mass Spectrometric System for Routine Measurements of Helium Isotopes and Tritium by the ^{3}He Ingrowth Method. Sitzungsberichte der Heidelberger Akademie der Wissenschaften, Mathematisch — naturwissenschaftliche Klasse 5. Abhandlung, pp. 241–279.

Benson, B.B., Krause, D., 1980. Isotopic fractionation of helium during solution: a probe of the liquid state. Journal of Solution Chemistry 9, 895–909.

Bersch, M., 1995. On the circulation of the northeastern North Atlantic. Deep-Sea Research I 42 (9), 1583–1607.

Borenäs, K.M., Lundberg, P.A., 1988. On the deep-water flow through the Faroe Bank Channel. Journal of Geophysical Research 93 (C2), 1281–1292.

Bullister, J.L., Weiss, R.F., 1988. Determination of CCl_3F and CCl_2F_2 in seawater and air. Deep-Sea Research 35, 839–853.

Bulsiewicz, K., Rose, H., Klatt, O., Putzka, A., Roether, W., 1995. A capillary-column chromatographic system for efficient chlorofluorocarbon measurement in ocean waters. Journal of Geophysical Research 103 (C8), 15959–15970.

Cunnold, D.M., Fraser, P.J., Weiss, R.F., Prinn, R.G., Simmonds, P.G., Miller, B.R., Alyea, F.N., Crawford, A.J., 1994. Global trends and annual releases of CCl_2F_2 and CCl_3F estimated from ALE/GAGE and other measurements from July 1978 to June 1991. Journal of Geophysical Research 99 (D1), 1107–1126.

Dickson, R.R., 1994. The production of North Atlantic Deep Water: sources, rates, and pathways. Journal of Geophysical Research 99 (C6), 12319–12341.

Doney, S.C., Bullister, J.L., 1992. A chlorofluorocarbon section in the eastern North Atlantic. Deep-Sea Research 39 (11/12), 1857–1883.

Doney, S.C., Jenkins, W.J., 1988. The effect of boundary conditions on tracer estimates of thermocline ventilation rates. Journal of Marine Research 46, 947–965.

Doney, S.C., Jenkins, W.J., 1994. Ventilation of the Deep Western Boundary Current and Abyssal Western North Atlantic: estimates from tritium and 3-He distributions. Journal of Physical Oceanography 24, 638–659.

Doney, S.C., Jenkins, W.J., Bullister, J.L., 1997. A comparison of ocean tracer dating techniques on a meridional section in the eastern North Atlantic. Deep-Sea Research I 44, 603–626.

Dreisigacker, E., Roether, W., 1978. Tritium and ^{90}Sr in north Atlantic surface water. Earth and Planetary Science Letters 38, 301–312.

Harvey, J.G., Theodorou, A., 1986. The circulation of Norwegian Sea overflow water in the eastern North Atlantic. Oceanologica Acta 9, 393–402.

Jenkins, W.J., 1988. The use of anthropogenic tritium and helium-3 to study subtropical gyre ventilation and circulation. Philosophical Transaction of the Royal Society of London A 325, 43–61.

Jenkins, W.J., 1998. Studying subtropical thermocline ventilation and circulation using tritium and ^{3}He. Journal of Geophysical Research 103 (C8), 15817–15831.

Jenkins, W.J., Clarke, W.B., 1976. The distribution of ^{3}He in the western Atlantic Ocean. Deep-Sea Research 23, 481–494.

Lee, A., Ellet, D., 1965. On the contribution of overflow water from the Norwegian Sea to the hydrographic structure of the North Atlantic Ocean. Deep-Sea Research 12, 129–142.

McCartney, M.S., 1992. Recirculating components to the deep boundary current of the northern North Atlantic. Progress in Oceanography 29, 283–383.

McCartney, M.S., Bennett, S.L., Woodgate-Jones, M.E., 1991. Eastward flow through the Midatlantic Ridge at 11°N and its influence on the abyss of the eastern basin. Journal of Physical Oceanography 14, 922–935.

Rhein, M., Fischer, J., Smethie, W.M., Smythe Wright, D., Weiss, R.F., Mertens, C., Min, D.H., Fleischmann, U., Putzka, A., 2001. Labrador Sea Water: pathways, CFC-inventory and formation rates. Journal of Physical Oceanography, in press.

Roether, W., Roussenov, V.M., Well, R., 1994. A Tracer study of the thermohaline circulation of the eastern Mediterranean. In: Malanotte-Rizzoli, P., Robinson, A.R. (Eds.), Ocean Processes in Climate Dynamics: Global and Mediterranean Examples. Kluwer, Dordrecht, pp. 371–394.

Saunders, P.M., 1994. The flux of overflow water through the Charlie-Gibbs Fracture Zone. Journal of Geophysical Research 99 (C6), 12343–12355.

Saunders, P.M., 1995. The flux of dense cold overflow water southeast of Iceland. Journal of Physical Oceanography 26, 85–95.

Schmitz, W.J.J., McCartney, M.S., 1993. On the North Atlantic circulation. Reviews of Geophysics 31 (1), 29–49.

Smethie Jr., W.M., Fine, R.A., Putzka, A., Jones, E.P., 2000. Tracing the flow of North Atlantic Deep Water using chlorofluorocarbons. Journal of Geophysical Research 105 (C6), 14297–14323.

Swift, J.H., 1984. The circulation of the Denmark Strait and Iceland–Scotland overflow waters in the North Atlantic. Deep-Sea Research 31, 1339–1355.

Sy, A., Rhein, M., Lazier, J.R.N., Koltermann, K.P., Meincke, J., Putzka, A., Bersch, M., 1997. Surprisingly rapid spreading of newly formed intermediate waters across the North Atlantic Ocean. Nature 386, 675–679.

Thiele, G., 1985. Ein kinematisches Boxmodell zur Auswertung der Verteilung anthropogener Spurenstoffe in der Warmwasserspäre des Nordostatlantik. Ph.D. Thesis, Naturwissenschaftlich-Mathematische Gesamtfakultät, Ruprechts-Karls-Universität, Heidelberg, 92pp.

Tsuchiya, M., Talley, L.D., McCartney, M.S., 1992. An eastern Atlantic section from Iceland southward across the equator. Deep Sea Research 39, 1885–1917.

van Aken, H.M., Becker, G., 1996. Hydrography and through-flow in the north-eastern North Atlantic Ocean: the Nansen Project. Progress in Oceanography 38, 297–346.

van Aken, H.M., de Boer, C.J., 1995. On the synoptic hydrography of intermediate and deep water masses in the Iceland Basin. Deep-Sea Research I 42 (3), 165–189.

Walker, S.J., Weiss, R.F., Salameh, P.K., 2000. Reconstructed histories of the annual mean atmospheric mole fractions for the halocarbons CFC-11, CFC-12, CFC-113 and carbon tetrachloride. Journal of Geophysical Research 105 (C6), 14285–14296.

Warner, M.J., Weiss, R.F., 1985. Solubilities of chlorofluorocarbons 11 and 12 in water and seawater. Deep-Sea Research 32, 1485–1497.